

Comparing accuracy and runtime of simulation to the measurements in a real grid for the control of a grid-connected PV inverter

Agknaton Bottenberg, Jos Knockaert, Jan Desmet
Ghent University, Campus Kortrijk, Belgium
Agknaton.Bottenberg@ugent.be

Abstract— The proposition for this study is to assess how much simulation results can differ from real measurements on the implementation of a control strategy for a grid-connected PV inverter. The system is simulated in Matlab/Simulink and experimentally evaluated on a real low-voltage distribution grid. The PV inverter is implemented using a power-hardware-in-the-loop platform running the control algorithm. The influence of linear and nonlinear loads and the interaction with another distributed energy resource operating on the same grid is quantified both in simulation and in the measurements. Finally, the control strategy is applied and the results for simulation and experimental setup are shown.

Index Terms—power system control; distributed power generation; renewable energy sources; digital control

I. INTRODUCTION

An increased penetration of Distributed Energy Resources (DER) brings many technical challenges to the operation of distribution systems such as overvoltage, power quality, protection and stability issues [1]. Some of these issues can be solved and new functionalities can be achieved by control strategies applied to the grid operation [2][3] or independently in the converters [4]. Control algorithms can be evaluated in a simulation environment and/or in an experimental setup before deployment.

Simulation is an important design tool for the development of control strategies for photovoltaic (PV) inverters, storage units, demand response, etc. Through simulation one can conveniently validate and optimize the control strategy, estimate the control parameters, assess the stability criteria, predict the system behavior and demonstrate the performance of the proposed strategy. The results are as accurate as the models and the computational methods. To have the results within a reasonable timeframe one must adapt the complexity of the models to the currently available computational tools, making a trade-off between runtime and accuracy. For example, converters with power electronics can be modelled with SPICE level simulation, piecewise linear approximation or average voltage models. Different modelling yields different results, usually within a tolerance margin. Measurements can be different than simulations even in steady-state, e.g. when connection resistances are not considered and offer a significant voltage drop.

Experimental evaluation of control algorithms on public low-voltage (LV) distribution grids with DER, on the other hand, have a few challenges of its own. It's difficult to ensure repeatability, interruptions to the operation are problematic to the users, installation and maintenances depend on user's availability and the distances between units may complicate the measurements, to name a few challenges. Laboratory tests with only loads and a power supply might provide some interesting results but usually are not able to fully replicate distribution grid behavior.

In this paper, the same control strategy is evaluated experimentally and with simulation models. The control strategy is a voltage-based droop control that acts over the injected power of a PV inverter. For the experimental evaluation, the control is implemented in a power-hardware-in-the-loop (PHIL) platform, connected to a real grid composed of 18 consumer/prosumer units. The interaction with linear loads, nonlinear loads and another PV inverter on the same system is evaluated. Incandescent lamps are used as linear loads and compact fluorescent lamps (CFL) as nonlinear loads. The simulation setup replicates the same system in Simulink.

The system under study is presented in section II. Section III describes how the system was implemented both experimentally and in simulation. The results from simulations and measurements are compared in section IV and section V discusses the results.

II. THE SYSTEM UNDER STUDY

A control strategy test case and a grid topology were chosen to provide a consistent scope for comparison between simulation and experimental measurements. The available infrastructure, the adequate complexity to be able to separate control action from grid reaction and relevance for future work within our research group were considered. The control test cases are based on the evaluation of a voltage-based droop control algorithm for PV inverters. The grid topology includes a connection of 18 houses in a region of considerable penetration of domestic PV production. The details are given below.

A. Voltage-based droop control

In the context of energy grids with DER, overvoltage is one of the main concerns. The surplus of available energy in the grid due to high energy production combined with low energy demand can lead to overvoltage. One of the possible solutions for this problem is active power curtailment (APC), which means to limit PV production when overvoltage is imminent. The APC in DER can be done in two ways. The first one is called hard-curtailment and means to disconnect the producing unit completely from the grid when the voltage reaches a certain threshold. This method can cause oscillations and even system failure due to the sudden disconnection of multiple producers [5][6]. The second method is to perform a gradual APC according to a droop-curve as shown in Fig. 1[5],[7]. In this method, the relationship between the injected power and the available power is a function of the voltage at the point of connection with the grid as follows:

$$p_{dc} = \begin{cases} p_{dc}^{DER}, & \text{if } v_g \leq v_{cpb} \\ p_{dc}^{DER} \left(1 - \frac{v_g - v_{cpb}}{v_{max} - v_{cpb}} \right), & \text{if } v_{cpb} < v_g < v_{max} \\ 0, & \text{if } v_g > v_{max} \end{cases}$$

where p_{dc} is the power injected into the grid, p_{dc}^{DER} is the available power from the source, v_g is the rms voltage at the grid connection, v_{cpb} is the constant power band voltage limit and v_{max} is the maximum allowable 10 minutes mean rms voltage in the grid as per EN50160 standard[8]. Instantaneous rms voltage is used in this work to speed up the tests.

B. Grid topology and test setup

Although the experimental grid can be easily configurable via software between different topologies (e.g. series, branch and meshed) a series grid topology was selected for this study. The reason is to maximize the impact of the DER on the grid voltage, by locating the controlled PV inverter unit at the end of the feeder. The grid can be composed of up to 18 consumer/prosumer units, with single-phase or 3-phase connection to the feeder. There are 464m of feeder cable between the power supply and the point of connection for house 17. Between the point of connection for house 17 and the point of connection for house 18 there are 15m of feeder cable. A simplified view of the test grid is shown in Fig. 2. The voltage-based droop control is implemented on a PV inverter installed at house 18. A set of selectable loads is connected to houses 17 and 18. House 17 has also a commercial PV inverter fed by a

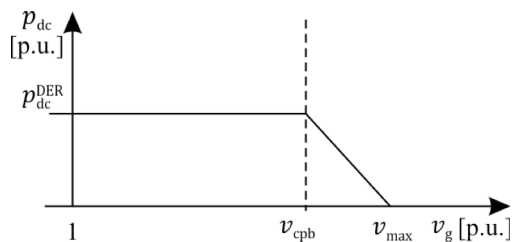


Fig. 1. Voltage-based droop control curve. The injected power is a function of the grid voltage.

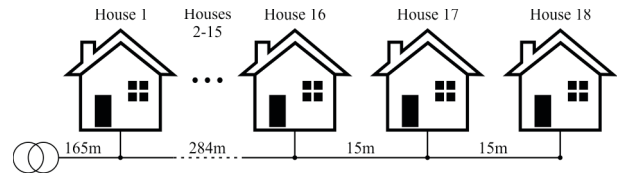


Fig. 2. Simplified view of the grid topology with 18 units ("houses"). The tests were performed controlling loads and PV production in houses 17 and 18.

dc power supply. A list of selectable loads and DER used for the tests is shown in Table I.

With this test setup, the following tests were performed both in simulation and experimental evaluation for later comparison:

1. 100% to 0% of linear loads at houses 17 and 18, without PV generation, $V_{source}=230V$;
2. 100% to 0% of nonlinear loads at houses 17 and 18, without PV generation, $V_{source}=230V$;
3. 100% to 0% of PV generation at house 17, without droop-control action, $V_{source}=230V$;
4. 100% to 0% of PV generation at house 18, without droop-control action, $V_{source}=230V$;
5. 100% to 0% of linear loads at houses 17 and 18, with droop-control action at house 18, $V_{source}=243V$;
6. 100% to 0% of nonlinear loads at houses 17 and 18, with droop-control action at house 18, $V_{source}=243V$;
7. 100% to 0% of PV generation at house 17, with droop-control action at house 18, $V_{source}=243V$;
8. Step from 230V (nominal) to 207V (-10% nominal) and ramp up to 253V (+10% nominal) with droop-control action at house 18.

Tests 1-4 are for basic comparison between simulation results and measurements. Tests 5-7 are to investigate the impact of loads and generation close to the PV running the control algorithm. Test 8 is to exercise the control strategy over its full action range. The simulation models, experimental setup and methodology will be further detailed in the next sections. The nominal values are $230V_{phase}/400V_{line}$ @ 50Hz.

III. IMPLEMENTATION OF THE TESTS

A. Experimental setup

The experimental part of this work was performed in the freely programmable interactive LV-grid of EELab Lemcko, shown in Fig. 3. The grid can be fed by the MV/LV transformer or a three-phase 240kVA freely programmable power-supply. The distribution feeder is composed by 600m of underground

TABLE I
DER AND LOADS FOR THE TESTS

House	Loads	DER
1-16	No independent loads. Voltage influence emulated by ac source voltage	No independent generation. Voltage influence emulated by ac source voltage
17	0-12 200W incandescent lamps; 0-12 15W CFLs	5kVA PV inverter with up to 3600W input power available
18	0-12 200W incandescent lamps; 0-12 15W CFLs	15kVA PV inverter with up to 3120W input power available



Fig. 3. The experimental grid laboratory. Each of the 18 numbered cabinets represents a domestic consumer.

cables that can be configured in 7 different grid topologies, selected by software. An extensive description of the programmable grid is presented in [9].

For this work, the houses are connected to the feeder in single phase with 25mm^2 cables and the feeder is supplied by the 240kVA programmable three-phase power supply.

The loads and DER were described in Table I. The lamps can be individually switched on and off and are grouped on a panel board as can be seen in Fig. 3.

The PV inverter connected to house 17 is a commercial single-phase 5kVA unit fed by a programmable dc source. The dc source emulates a set of PV panels and can provide up to 3.6kW as 450V/8A.

The voltage-based droop control is implemented in the UGK-PM15F42 PHIL platform from Triphase [10] with a control rate of 16kHz. Control rate is equal to 1/cycle time. This platform is composed by a Real-Time Target (RTT) computer, two power modules (15kVA three-leg programmable inverters) and voltage/current sensors. The connection to the grid and internal configurations are performed via a network of actuators and sensors. An LCL filter is implemented at the outputs of the power modules. The RTT runs a compiled version of the Simulink model that implements the desired control. Constants, displays and scopes of the model can be accessed during runtime, allowing parameter configuration and system monitoring in real-time. It is also possible to create logs of internal signals up to the sampling rate for later analysis.

The PHIL platform is connected to the grid in single-phase. The PV generation is emulated by a programmable dc source, providing up to 3120W as 400V/7.8A

Measurements are made with a PM3000A power analyser, with an interval of 3s between reads. Active power, reactive power, rms voltage and rms current are measured.

B. Simulation model

The test setup is modelled using Simulink. The programmable power supply is modelled as a three-phase ac source with an amplitude set input. This input is used in the step and ramp voltage test.

The feeder cabling is modelled according to the cable specifications, with $\sim 0.2\Omega/\text{km}$ resistance and $\sim 2\text{mH}/\text{km}$ inductance. The 25mm^2 cabling from feeder to house has $\sim 0.7\Omega/\text{km}$ and $\sim 2\text{mH}/\text{km}$.

The linear loads are modelled as 264.5 Ω resistors to reflect the 200W incandescent lamps. The nonlinear loads were modelled using the CFL model presented in [11].

The PV inverters are modelled based on [12]. The MPPT control was removed and replaced by a direct control of I_d and I_q based on the available power and nominal values. The voltage-based droop control is implemented on top of the PV inverter model for house 18. To optimize the runtime, the average voltage mode is used for the voltage source converter. This change allows the simulation model to run at the same sample rate as the PHIL platform, 16kHz.

An additional nonlinear constant load is added to house 18's model to represent the base power drained by the PHIL platform. The simulations ran in Matlab 2016b on a i5 intel PC with 8GB of RAM, the OS is Windows 10.

IV. COMPARISON OF RESULTS

A. Base test cases without droop control

To establish a base comparison between simulation and measurements, tests 1-4 from section II.B were performed. For the load sweeping the tests begin with all lamps on, with a warm-up time of 10 minutes for the CFLs. The lamps are then switched off one by one with an interval of 6-12 seconds between lamps. First the lamps at house 18, then the lamps at house 17. For the tests with PV injection the total available power was divided in 8 equal steps, from maximum power to zero.

A sensitivity analysis is performed to compare simulations with experimental results in a numeric and time invariant base. Using the non-linear least squares method, the simulation results and measurements are fitted to the following equation:

$$V_{Hn} = m_1 \cdot P_{H17} + m_2 \cdot P_{H18} + a \quad (1)$$

where V_{Hn} is the rms at house n (17 or 18); m_1 is the linear coefficient that relates P_{H17} to V_{Hn} ; m_2 is the linear coefficient that relates P_{H18} to V_{Hn} ; P_{H17} and P_{H18} are active power at house 17 and house 18, respectively; and a is the voltage at no-load. The active power is positive when the house is consuming and negative when the house is injecting power into the grid.

The results are presented in Table II. The voltages at each house are evaluated separately, so (1) is applied twice for each curve fit. The column "error_{max}" indicates the maximal error in percent between the fitted curve and the actual results. Column "average runtime" shows the average execution time for each test case. For experimental evaluation, this value is 1 second/second and, for simulation, is the total simulation runtime divided by the simulated time. The cells marked with "n/a" indicates coefficients that don't contribute to the result. For the PV injection test cases, no power was consumed or injected at the other house, so the respective P_{Hn} is always zero during that test case. The coefficients presented in this table relate the

TABLE II
RELATIONSHIP BETWEEN ACTIVE POWER AND RMS VOLTAGE FOR SIMULATION AND EXPERIMENTAL EVALUATION

	Results for V_{H17}				Results for V_{H18}				Average runtime (s/s)
	m_1	m_2	a	error _{max} (%)	m_1	m_2	a	error _{max} (%)	
Linear loads	-8.528E-04	-7.900E-04	2.300E+02	4.734E-03	-7.754E-04	-8.866E-04	2.300E+02	4.833E-03	21.9087
	-1.906E-03	-9.684E-04	2.311E+02	1.196E-01	-9.897E-04	-2.082E-03	2.311E+02	8.164E-02	1
Nonlinear loads	-7.234E-04	-6.505E-04	2.300E+02	1.401E-03	-6.505E-04	-7.388E-04	2.300E+02	1.487E-03	23.4977
	-2.203E-03	-6.892E-04	2.311E+02	6.203E-02	-8.434E-04	-2.121E-03	2.311E+02	6.752E-02	1
PV injection at house 17 only	-8.343E-04	n/a	2.300E+02	1.205E-02	-7.586E-04	n/a	2.300E+02	1.159E-02	17.6066
	-1.788E-03	n/a	2.311E+02	1.267E-01	-9.559E-04	n/a	2.311E+02	7.058E-02	1
PV injection at house 18 only	n/a	-7.610E-04	2.301E+02	7.359E-03	n/a	-8.558E-04	2.301E+02	8.334E-03	22.7549
	n/a	-9.385E-04	2.312E+02	8.518E-02	n/a	-1.752E-03	2.312E+02	8.483E-02	1

power values used in the test cases with the voltages measured on the grid. This means that it's possible to plot the resulting power-voltage curves for test cases 1-4 just applying the respective coefficients and output powers, as described in the test description, into (1).

Some consideration can be made from Table II. The coefficient a corresponds to the no-load voltage, so roughly the power supply voltage. This value is closer to the nominal voltage of 230V in simulation than in experimental evaluation. The reason is that the total power used (~ 5 kW) is too low compared to the nominal power for the power supply (3×80 kVA), so the output voltage is a bit higher. Another point is the coefficient m that relates P_{Hn} to V_{Hn} (for the same house). The m value from measurements is more than 2 times bigger than the m from simulations. This means that the resistance between the connection to the feeder and the loads/PV inverters is higher than modelled. This increased resistance is caused by the connections and contactors between the feeder and the output connections. These contactors are used to select the wiring between the different possible connection configurations for each house e.g. the cable width for the house installation between 10, 16 and 25mm². The effect of this increased resistance is visible in the next test cases. The other m coefficient, that quantifies the sensitivity of grid voltage to the power at the neighbor's house, is consistent between measurements and simulations.

B. Evaluation of the impact of close loads and DER

The test cases 5-7 from section II.B were performed to evaluate the voltage-droop based control interaction with loads and DER generation at the same house and in neighbor houses. It

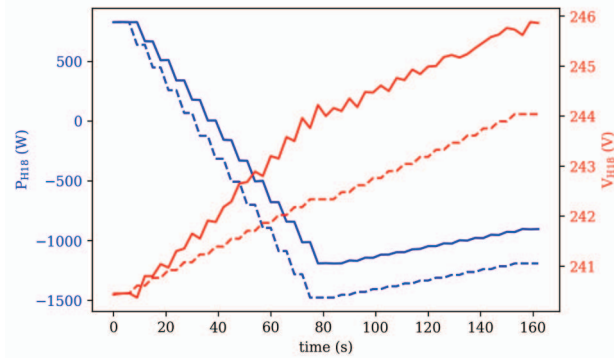


Fig. 4. Control response to linear load variation, measured on house 18. Solid lines are the measured and dashed lines the simulated results.

is assumed that there is a strong DER penetration and overproduction, increasing the nominal grid voltage to 243V (conveniently at the midpoint of the droop curve).

Fig. 4 shows test case 5. From 0 to 80 seconds the incandescent lamps from house 18 are gradually switched off. The increased resistance mentioned in the previous section is clearly observed as the grid voltage slope is steeper for measurement values and voltage difference gets bigger as PV injects more power into the grid. After 80 seconds the droop control is observed in the active power curve. As the voltage increases because of the load being reduced in house 17, the active power injection decreases linearly. The average runtime is 23.0238 seconds/second.

Fig. 5 shows test case 6. The overall response in time is similar to the previous test case, although the power and voltage steps are proportionally smaller. The average runtime is 23.3939 seconds/second.

The results from test case 7 are presented in Fig. 6. At the beginning of the test the grid voltage already is quite high. With a grid voltage of 248V the droop control limits the output power to 27% of the available power. As house 17 starts decreasing its DER production, the grid voltage also decreases. The rate of decrease is limited though by the control action, that makes house 18 inject more power as the grid voltage decreases. It is important to notice that there is a ~ 2 V difference between simulation and measurements. This difference is mainly due to the higher resistance at the connection between the PHIL platform and the feeder. The average runtime is 20.3055 seconds/second.

C. Step and ramp test

Finally, the response to a voltage step and ramp is shown in Fig. 7. Again, the effect quantified in the sensitivity coefficients difference can be seen, as the slope of voltage variation

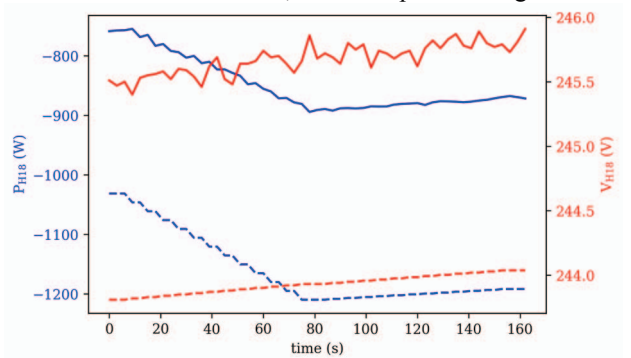


Fig. 5. Control response to nonlinear load variation, measured on house 18. Solid lines are the measured and dashed lines the simulated results.

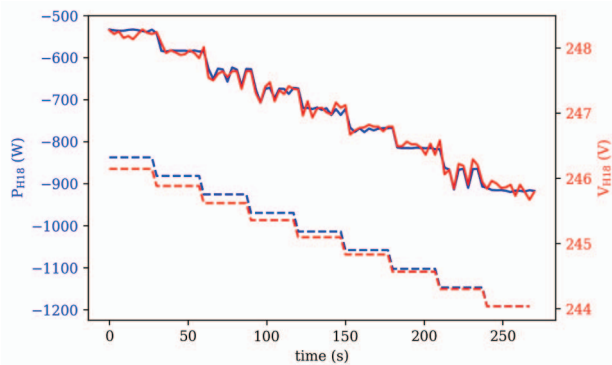


Fig. 6. Control response to PV injection at house 17, measured on house 18. Solid lines are the measured and dashed lines the simulated results.

is steeper for measurements than simulations. The step response at the beginning of the test shows no overshoot neither for measurement nor simulation. The reason is in the design of the controller, that limits sudden changes at the output to prevent instability. Faster control designs could present oscillations and interactions with the grid that differ between simulation and measurements. Another feature in the voltage curve is the change of slope when the droop control crosses the constant power band voltage limit (v_{cpb}). The inverter injects constant power up to 1.02 p.u.. As the voltage crosses that threshold, the injected power decreases linearly with the voltage. The combined action of the supply voltage ramp with the voltage-droop control curve from the PV inverter changes the slope of the voltage ramp at the point of connection with the feeder. The average runtime is 17.8523 seconds/second.

V. FINAL CONSIDERATIONS

The value of simulation resides on the abstraction of all the layers below the application level, managing the complexity and making the need for physical implementation nonessential for system evaluation. New control algorithms for DER can be easily evaluated and improved with adequate tools and models. However, experimental validation is required to ensure proper operation of the controller before deployment of a commercial product. In a way, the complexities of the grid become transparent to the developer, just like the lower levels of abstraction in the simulation models. Nonlinearities, interactions between components and instabilities can be evaluated through their measurable effects without the need for deep complex modeling of their causes. A better approach can be using both simulation and measurements and keep them close. If the simulated system is modelled from the beginning to reflect an available real setup, the later experimental validation is facilitated as the test cases can be developed and evaluated based on a consistent system model. Complex blocks can have simplified versions to speed-up initial development. When accuracy becomes more important than speed, these blocks can be replaced by their detailed versions. A PHIL platform is an important link in such approach with power systems, to reduce the implementation overhead of prototyping hardware and to speed-up development cycles. As seen in this paper with the resistance at the houses' connection, measurements can provide information

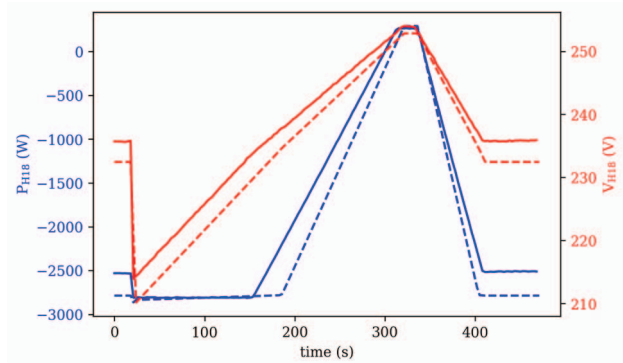


Fig. 7. Control response to grid voltage step and ramp, measured on house 18. Solid lines are the measured and dashed lines the simulated results.

that could improve the accuracy of the models. The opposite is also true, a simulation can inspire improvements to the experimental setup. Some inspirations from this work to facilitate future work are to automate the load switching and to control the measurement devices at runtime using the RTT computer.

REFERENCES

- [1] J. A. P. Lopes, N. Hatziaargyriou, J. Mutale, P. Djapic, and N. Jenkins, "Integrating distributed generation into electric power systems: A review of drivers, challenges and opportunities," *Electr. Power Syst. Res.*, vol. 77, no. 9, pp. 1189–1203, Jul. 2007.
- [2] J. M. Guerrero, M. Chandorkar, T. L. Lee, and P. C. Loh, "Advanced control architectures for intelligent microgrids - part I: Decentralized and hierarchical control," *IEEE Trans. Ind. Electron.*, vol. 60, no. 4, pp. 1254–1262, Apr. 2013.
- [3] J. M. Guerrero, P. C. Loh, T. L. Lee, and M. Chandorkar, "Advanced control architectures for intelligent microgrids - part II: Power quality, energy storage, and ac/dc microgrids," *IEEE Trans. Ind. Electron.*, vol. 60, no. 4, pp. 1263–1270, Apr. 2013.
- [4] J. Rocabert, A. Luna, F. Blaabjerg, and P. Rodríguez, "Control of power converters in AC microgrids," *IEEE Trans. Power Electron.*, vol. 27, no. 11, pp. 4734–4749, Nov. 2012.
- [5] T. L. Vandoorn, J. D. Kooning, B. Meersman, and L. Vandevelde, "Voltage-based droop control of renewables to avoid on-off oscillations caused by overvoltages," *IEEE Trans. Power Deliv.*, vol. 28, no. 2, pp. 845–854, Apr. 2013.
- [6] E. Demirok, P. C. González, K. H. B. Frederiksen, D. Sera, P. Rodriguez, and R. Teodorescu, "Local reactive power control methods for overvoltage prevention of distributed solar inverters in low-voltage grids," *IEEE J. Photovolt.*, vol. 1, no. 2, pp. 174–182, Oct. 2011.
- [7] D. V. Bozalakov, T. L. Vandoorn, B. Meersman, G. K. Papagiannis, A. I. Chrysochos, and L. Vandevelde, "Damping-based droop control strategy allowing an increased penetration of renewable energy resources in low-voltage grids," *IEEE Trans. Power Deliv.*, vol. 31, no. 4, pp. 1447–1455, Aug. 2016.
- [8] EN50160, "Voltage characteristics of electricity supplied by public electricity networks." European Committee for Electrotechnical Standardization (CENELEC), 2010.
- [9] J. Desmet, B. Verhelst, L. Vandevelde, and C. Debruyne, "Test field for LV distribution systems," in *22nd International Conference and Exhibition on Electricity Distribution (CIRED 2013)*, 2013, pp. 1–4.
- [10] Triphase NV, "Power Modules," *Triphase.com*. [Online]. Available: <https://triphase.com/products/power-modules/>. [Accessed: 12-Jun-2017].
- [11] J. Molina and L. Sainz, "Model of Electronic Ballast Compact Fluorescent Lamps," *IEEE Trans. Power Deliv.*, vol. 29, no. 3, pp. 1363–1371, Jun. 2014.
- [12] Mathworks, "Single-Phase, 240 Vrms, 3500 W Transformerless Grid-Connected PV Array - MATLAB & Simulink Example." [Online]. Available: <https://nl.mathworks.com/help/physmod/sps/examples/single-phase-240-vrms-3500-w-transformerless-grid-connected-pv-array.html>. [Accessed: 12-Jun-2017].